

Effects of Relativistic Dynamics in $pp \longrightarrow pp\pi^0$ near Threshold

J. Adam, Jr.^{1,2}, Alfred Stadler³, M. T. Peña^{3,4}, Franz Gross^{1,5}

¹*Jefferson Lab, 12000 Jefferson Avenue, Newport News, VA 23606*

²*Institute of Nuclear Physics, Řež n. Prague, CZ-25068, Czech Republic*

³*Centro de Física Nuclear da Universidade de Lisboa, 1699 Lisboa Codex, Portugal*

⁴*Departamento de Física, Instituto Superior Técnico, 1096 Lisboa Codex, Portugal*

⁵*Department of Physics, College of William and Mary, Williamsburg, Virginia 23185*

(March 17, 2018)

Abstract

The cross-section for threshold π^0 production in proton-proton collisions is evaluated in the framework of the covariant spectator description. The negative energy intermediate states are included non-perturbatively and seen to yield a considerably smaller contribution, when compared to perturbative treatments. A family of OBE-models with different off-shell scalar coupling is considered.

I. INTRODUCTION

The reaction $pp \rightarrow pp\pi^0$ near threshold is very sensitive to the description of the NN -interaction and to π^0 production mechanisms. Due to the underlying chiral symmetry both the single-nucleon term and the pion-rescattering contribution are suppressed near threshold [1–3]. The transition amplitude then results from a delicate interference between these and various additional contributions of shorter range [2,4–10]. The relevance and relative importance of various reaction mechanisms, in particular the short range ones, has not yet been firmly established. A treatment of these mechanisms consistent with the NN interactions employed in the description of the final and initial state is needed to clarify the large model dependence. Moreover, the magnitude of the transferred hadronic momentum, which is typically $p/m \sim \sqrt{\mu/m} \sim 0.4$, calls for a relativistic approach.

In this letter we re-examine the single-nucleon term using the covariant spectator description [12–14] for both the production mechanism and for the initial and final state pp interaction. The pion emission from a single proton is described by the Feynman diagrams of Figure 1. The OBE spectator models [13] allow a direct covariant evaluation of diagrams (a)-(c). Dynamically, these are the only model-independent contributions. There might be additional reaction mechanisms, in particular involving pion rescattering, such as diagram (d). They have not yet been included in our calculations. The intermediate state nucleons in diagrams (a)-(c) can propagate with positive and negative energy. We will split the contribution of these diagrams into amplitudes a^\pm, b^\pm and $c^{\pm,\pm}$ with the superscript indicating the sign of the energy of the off-shell nucleon after and/or before the pion emission.

Our approach differs crucially from earlier ones in two aspects. Firstly, it includes non-perturbatively diagrams with intermediate negative-energy nucleons. In perturbative approaches these contributions are simulated by the inclusion of effective meson-exchange operators acting in two-nucleon space (their contributions are often called “Z-diagrams”). More specifically, one takes the amplitudes a^- and b^- (with the nucleons in the initial and final state on-shell) to the lowest order in $v/c \sim p/m$, replacing the NN interaction by a single one-meson exchange, usually taking into account only the most important meson exchanges. Written in the space of two-component Pauli spinors these amplitudes are identified with effective pion-production meson-exchange operators and their expectation values are then calculated with conventional nuclear wave functions. These transition amplitudes simulate those contributions of the diagrams a^-, b^-, c^{+-} and c^{-+} for which the transition to negative-energy nucleons occurs only once.

In previous perturbative calculations [2–10] the most important contributions to the Z-diagram operator were found to be the exchanges of σ , ω , and π mesons. It has been shown [7] that the pion Z-graph yields a much smaller contribution than the σ and ω diagrams. It is often considered together with other model dependent off-shell pion-rescattering processes [2,9,10]. In v/c -expansion calculations, the σ and ω Z-graphs were found to dominate the short range reaction mechanisms and provide contributions essential for the explanation of the data. In contrast, in the present covariant calculations we obtained significantly smaller contributions from terms with negative-energy nucleons.

Secondly, the NN -models considered recently [14] include non-minimal dynamical effects produced by off-shell scalar-nucleon coupling, scaled by a parameter ν :

$$\Gamma_s(p', p) = g_s \left\{ 1 + \frac{\nu_s}{2m} [\not{p}' + \not{p} - 2m] \right\}, \quad (1)$$

with $\nu_\sigma = -0.75\nu$, and $\nu_\delta = 2.6\nu$. Both NN -observables and the triton binding energy appear to be rather sensitive to this off-shell extension, hence it is very interesting to find out if it also works favorably in the considered reaction. Taking only diagrams (a) and (b) for σ and ω exchange in Born approximation, we, indeed, have found a rather strong dependence on the parameter ν , mainly due to the cancellation between σ and ω terms. However, the variation is much weaker when the full interaction is included.

II. THEORETICAL DESCRIPTION

Near threshold the reaction is dominated by transition between initial 3P_0 and final 1S_0 pp partial waves; only these are considered in our calculations. The total cross section is given [15] in terms of the covariant transition amplitude \mathcal{M} :

$$\sigma[\mu b] = \frac{10^4(\hbar c)^2}{(2\pi)^5} \frac{m^2}{4pE} |\overline{\mathcal{M}}|^2 \rho(T_{lab}), \quad (2)$$

$$|\overline{\mathcal{M}}|^2 = \frac{1}{4} \sum_{\lambda'_1, \lambda_1, \lambda'_2, \lambda_2} \mathcal{M}_{\lambda'_1 \lambda_1, \lambda'_2 \lambda_2} \mathcal{M}_{\lambda'_1 \lambda_1, \lambda'_2 \lambda_2}^*, \quad (3)$$

where m is the nucleon mass; $p, E = \sqrt{p^2 + m^2}$ are the relative momentum and energy in the initial state; $\rho(T_{lab})$ is the phase space density, T_{lab} is the kinetic energy of the incoming proton. The amplitude \mathcal{M} and the phase space density ρ have dimensions MeV^{-3} , and MeV^4 , respectively. The helicity transition amplitude $\mathcal{M}_{\lambda'_1 \lambda_1, \lambda'_2 \lambda_2}$ is calculated from the Feynman rules as defined in [15]. For the partial waves considered, there is only one independent helicity amplitude, $\mathcal{M}_{++,+}^{J=0} = i \exp(i\delta_3(E)) \mathcal{M}$, with $\delta_3(E)$ being the 3P_0 phase shift.

The NN -interactions [13] used in our calculations were fitted to np -data and the effect of the Coulomb interaction is not included. It would suppress the cross section at threshold by about 40%. It has been shown [5], that using a constant amplitude in (2) results in a roughly quadratic dependence of σ on T_{lab} , clearly at variance with the experimental data (Fig. 2).

The most pronounced energy dependence of the total transition amplitude comes from the energy dependence of the final state 1S_0 interaction. We deal with it in an approximate way similar to that employed in [16]: we assume that the energy dependence of the final state scattering matrix is well approximated by the energy dependence of the corresponding on-shell NN scattering matrix $M(p) = M(p, p)$,

$$M(p', p) = M(0, p) \frac{M(p', p)}{M(0, p)} \approx M(0, p) \frac{M(p')}{M(0)}. \quad (4)$$

Expressing $M(p')$ in terms of the 1S_0 phase-shift δ_1 and $M(0)$ in terms of the singlet scattering length a_s , one obtains

$$M(p', p) \approx -\exp(i\delta_1(E')) \frac{m \sin(\delta_1(E'))}{E' (a_s p')} M(0, p), \quad (5)$$

with p', E' being the relative momentum and energy of the final pp state. Accordingly, the square of the transition amplitude contains the energy-dependent factor

$$\xi(p') = \left(\frac{m}{E'}\right)^2 \frac{\sin^2(\delta_1(E'))}{(a_s p')^2}. \quad (6)$$

We introduce it into (2) by replacing

$$\begin{aligned} \rho(T_{lab}) \longrightarrow \rho(\xi, T_{lab}) &= \int \frac{m}{E_1} d\vec{p}'_1 \frac{m}{E_2} d\vec{p}'_2 \frac{d\vec{q}}{2\omega_q} \\ &\xi(p') \delta^{(4)}(p_1 + p_2 - p'_1 - p'_1 - q). \end{aligned} \quad (7)$$

The difference between $\rho(1, T_{lab})$ and $\rho(\xi, T_{lab})$ is illustrated in Fig. 2. The approximation introduced in (4) implies for the Heitler R -matrix $R(p', p)/R(p') \approx R(0, p)/R(0)$. Figure 3 demonstrates the quality of this assumption about the energy dependence of the off-shell R -matrices. The curves corresponding to different energies would coincide in case the factorization describing the energy dependence of the half-off-shell NN amplitudes $R^{++}(p', p)$ were exact.

We note that we did not employ the effective range approximation for the final state scattering amplitude as it was used in Ref. [4]; it was found in Ref. [5] to artificially increase the cross section. Since the approximation (4) allows for a very good description of the energy dependence of the data, it can be used to extract the value of the threshold amplitude \mathcal{M} . A fit to the data of Ref. [16] yields a value

$$|\mathcal{M}_{exp}| = 30.5 \times 10^{-7} \text{MeV}^{-3}, \quad (8)$$

which is to be compared with our calculations summarized in Table I. A similar fit employing the unmodified phase space density with an unrealistic energy dependence of the cross section leads to a much smaller value $|\mathcal{M}_{exp}| = 5.0 \times 10^{-7} \text{MeV}^{-3}$.

III. RESULTS AND CONCLUSION

Table I shows in detail the contributions of diagrams (a)-(c) for several models that differ in their off-shell parameter ν . The best fit to the NN data was obtained [14] by models with ν in the range 1.5 – 2.0. From the models listed in the table, the one with $\nu = 1.6$ yields the triton binding energy closest to its experimental value [14].

The amplitudes are, in general, complex numbers, but we can subtract the two contributions from diagram (c) which correspond to having both intermediate nucleons on-shell either before or after pion is emitted, and add them to the amplitudes of diagrams (a) and (b), respectively. Then we arrive at new partial amplitudes that can be written as real numbers (which are given in Table I) times a common phase factor. However, one has to be cautious when comparing to other calculations that present results for the original diagrams. At threshold, the final state phase shift is zero and in terms of the real numbers A , B , and C the actual partial amplitudes are given as

$$\begin{aligned}
a^\pm &= A^\pm / \cos \delta_3 \\
b^- &= \exp(i\delta_3) B^- \\
c^{\pm,+} &= \exp(i\delta_3) (C^{\pm,+} + iA^\pm \tan \delta_3) \\
c^{\pm,-} &= \exp(i\delta_3) C^{\pm,-} .
\end{aligned} \tag{9}$$

The upper part of the table presents results of our covariant calculations. Diagram (c) dominates at threshold. Our results show a moderate dependence on the parameter ν and we observe that the amplitudes for the models with nonzero ν are somewhat enhanced. The largest value, at $\nu = 1$, is about 20 % larger than the smallest at $\nu = 0$. This translates into a more than 40 % variation in the total cross section. Although in itself it represents a sizeable effect, it is at this point not clear how much of it will survive in more complete calculations that would include other, model-dependent reaction mechanisms (such as that of diagram (d)).

Our total result is 2-3 times smaller than the fitted amplitude (8) for all models. The relativistic NN potentials [13] contain form factors for off-shell nucleons (sometimes called “sideways” form factors). For consistency we include them also in the pion emission vertex. They decrease the results by up to 10 % (see Table I). For reference and for comparison with perturbative results the total results without these form factors are also given (line “ no N ffs ”). The nucleon form factors are not included in our perturbative transition operators. It is difficult to take them into account consistently in v/c - expansion approaches, and the usual NN potentials and pion emission operators never consider them.

The last three lines of Table I list the usual perturbative results obtained with the same nucleon wave functions and with the meson parameters and meson-nucleon form factors consistent with the NN interaction employed. The first line gives the perturbative IA, to be compared with the subtotal $\mathcal{M}^+ = A^+ + C^{++}$ of covariant results. The perturbative result is somewhat larger, the difference between these numbers is due to the v/c -decomposition in the one-nucleon operator at threshold (in the covariant description it contains a factor $1/E$ compared to $1/m$ in the perturbative one) and to the presence of the off-shell nucleon form factors in the relativistic calculations.

The perturbative contribution of the Z-diagrams given in the second last line is to be compared to the sum of all terms with negative energy nucleon(s) in intermediate states: $\mathcal{M}^- = A^- + B^- + C^{+-} + C^{-+} + C^{--}$. We see that the perturbative result is more than 3 times as large as the covariant one. Notice also that the perturbative results would reproduce very well the experimental amplitude (8), though one should recall that Coulomb effects would suppress the cross section at threshold by about 40 %.

We do not consider here the model-dependent pion-production mechanisms, e.g., the pion-rescattering, and the $\rho-\omega-\pi$ diagram introduced in Ref. [2]. They can easily contribute by the same amount as the model independent nucleon Born diagrams considered so far. However, care should be taken to include them in a way consistent with the dynamics of the NN -interaction.

In conclusion, the sensitive cross section of π^0 production seems to be an ideal place to look for effects of relativistic dynamics. Our exploratory studies reported in this letter indeed lead to an assessment of the importance of “Z-diagrams” different from the traditional nonrelativistic ones. Our main conclusion is that such diagrams, when included in

a non-perturbative way, contribute differently than their non-relativistic limits taken perturbatively. A similar effect was reported in Ref. [17] for the elastic electron scattering on deuteron, but there it becomes noticeable at a momentum transfer ~ 1 GeV. Our present calculations in relativistic impulse approximation underestimate the data. In future calculations we plan to go beyond the threshold approximations and include pion rescattering contributions.

ACKNOWLEDGMENTS

J.A. and F.G. thank the Lisbon CFNUL theory group, and A.S. and M.T.P. thank the Jefferson Lab theory group, for the kind hospitality they received during their mutual visits. We wish to thank S. Coon, Ch. Hanhart, D.O. Riska, and U. van Kolck for helpful discussions on the subject. This work was supported by the DOE under contract number DE-FG05-88ER40435, by PRAXIS under contract number praxis/2/2.1/FIS/223/94, by CERN under contract number CERN/P/FIS/1101/96, and by JNICT under contract number BCC/4394/94.

REFERENCES

- [1] T. D. Cohen, J. L. Friar, G. A. Miller, and U. van Kolck, Phys. Rev. C **53**, 2661 (1996).
- [2] U. van Kolck, G. A. Miller, D. O. Riska, Phys. Lett. **B388**, 679 (1996).
- [3] B.- Y. Park, F. Myhrer, J. R. Morones, T. Meissner, and K. Kubodera, Phys. Rev. C **53**, 1519 (1996).
- [4] D. Koltun and A. Reitan, Phys. Rev. **141**, 1413 (1966).
- [5] G. Miller and P. U. Sauer, Phys. Rev. C **44**, R1725 (1991).
- [6] J. Niskanen, Phys. Lett. **B289**, 227 (1992).
- [7] C. J. Horowitz, Phys. Rev. C **48**, 2920 (1993).
- [8] T.-S. H. Lee and D. O. Riska, Phys. Rev. Lett. **70**, 2237 (1993).
- [9] E. Hernández and E. Oset, Phys. Lett. **B350**, 158 (1995).
- [10] C. Hanhart, J. Haidenbauer, A. Reuber, C. Schütz, and J. Speth, Phys. Lett. **B358**, 21 (1995).
- [11] R. Shyam and U. Mosel, nucl-th/9611013
- [12] F. Gross, Phys. Rev. **184** (1969) 1448; Phys. Rev. D **10** (1974) 223; Phys. Rev. C **26** (1982) 2203.
- [13] F. Gross, J. W. Van Orden and K. Holinde, Phys. Rev. C **45** (1992) 2094.
- [14] A. Stadler and F. Gross, Phys. Rev. Lett. **78**, 26 (1997).
- [15] J. D. Bjorken and S. D. Drell, Relativistic Quantum Mechanics, McGraw-Hill, New York, 1964.
- [16] H. O. Meyer et al., Nucl. Phys. **A539** 633 (1992).
- [17] M.J. Zuilhof and J.A. Tjon, Phys. Lett. **B84**, 31 (1979).

FIGURES

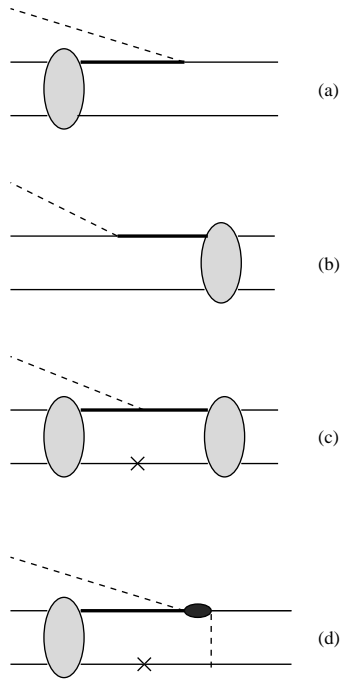


FIG. 1. The relativistic impulse approximation is defined by diagrams (a), (b), and (c). The shaded areas are NN scattering amplitudes. Diagram (d) is an example of the model dependent diagrams not included here. The thick lines represent off-shell nucleons, they can propagate with positive and negative energy.

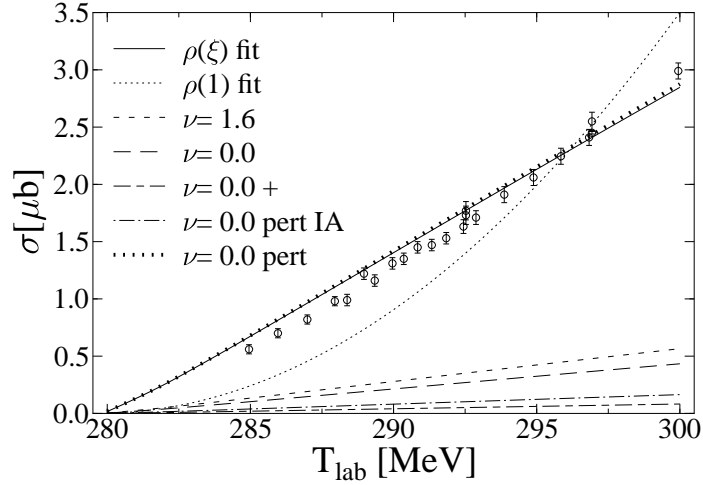


FIG. 2. Total cross section vs lab energy of incoming proton. The Indiana data [16] are shown with the best fits using unmodified $\rho(1)$ and modified $\rho(\xi)$ phase space densities, respectively. The curves labeled $\nu = 1.6$ and $\nu = 0.0$ are the full results of the covariant calculations. For the model with $\nu = 0.0$ we also show the cross section calculated with \mathcal{M}^+ only, labeled “ $\nu = 0.0 +$ ”, to be compared with the perturbative IA “ $\nu = 0.0, \text{ pert IA}$ ”. The full perturbative prediction “ $\nu = 0.0, \text{ pert}$ ” virtually coincides with the $\rho(\xi)$ fit.

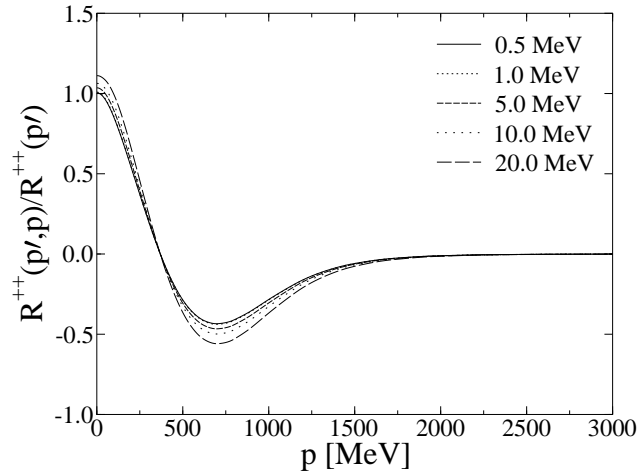


FIG. 3. Ratio of half off-shell and on-shell amplitudes of the model with $\nu = 1.6$ for various two-nucleon lab energies (in MeV) as a function of the off-shell momentum p .

TABLES

TABLE I. Amplitudes of diagrams (a), (b), (c) for several NN -interaction models. For diagrams (a) and (c) the amplitude is also separated into contributions due to positive and negative energy nucleons in the intermediate state(s). To diagram (b) at threshold only intermediate negative energy state contributes. $\mathcal{M}^+ = A^+ + C^{++}$, $\mathcal{M}^- = A^- + B^- + C^{+-} + C^{-+} + C^{--}$. The correspondence between the real numbers A, B , and C and the complex amplitudes of diagrams (a), (b), and (c), is explained in the text. The label “no N ffs” refers to the total covariant results with the off-shell nucleon form factors switched off. Perturbative results are denoted by “Pert.”. All amplitudes are given in units of 10^{-7} MeV^{-3} .

Diagram	$\nu = 0$	$\nu = 1.0$	$\nu = 1.6$	$\nu = 2.0$
A^+	1.11	-0.70	-1.08	-1.28
A^-	-1.44	-0.87	-0.04	0.68
A	-0.33	-1.58	-1.12	-0.60
$B = B^-$	-0.47	-0.55	-0.55	-0.54
C^{++}	-6.28	-6.06	-5.73	-5.62
C^{+-}	-5.42	-6.50	-6.41	-6.28
C^{-+}	0.56	0.42	0.19	0.02
C^{--}	0.06	0.06	0.04	0.01
C	-11.1	-12.1	-11.9	-11.9
\mathcal{M}^+	-5.17	-6.77	-6.81	-6.90
\mathcal{M}^-	-6.71	-7.44	-6.77	-6.11
Total	-11.88	-14.21	-13.57	-13.00
no N ffs	-12.64	-14.70	-13.91	-13.30
Pert. IA	-7.31	-8.72	-8.50	-8.48
Pert. Z-diag	-23.3	-24.6	-24.8	-23.7
Pert. total	-30.6	-33.3	-33.3	-32.2